

Fabrication of a pilot scale module of thin film composite hollow fiber membrane for osmotic pressure-driven processes

Chul Ho Park,¹ Sung Jo Kwak,¹ Jiyeon Choi,¹ Kangwon Lee,² Jung-Hyun Lee³

¹Jeju Global Research Center (JGRC), Korea Institute of Energy Research (KIER), 200 Haemajihae-ro, Gujwa-Eup Jeju Specific Self-Governing Province 63357, South Korea

²PHILOS Co. Ltd., B-1210, 60 Haan-ro, Gwangmyeong-Si, Gyeonggi-Do 14322, South Korea

³Department of Chemical & Biological Engineering, Korea University, 145 Anam-Ro, Seongbuk-Gu, Seoul 02841, South Korea

Correspondence to: C. H. Park (E-mail: chpark@kier.re.kr) and J.-H. Lee (E-mail: leejhyy@korea.ac.kr)

ABSTRACT: Polyamide thin film composite hollow fiber membranes have advantages in their unique structure compared to flat sheet membranes. This study examined interfacial polymerization methods for fabricating pilot scale hollow fiber membranes (membrane area: 1.2 m², number of hollow fiber strands: 1200). For use in osmotic pressure-driven processes, a one-pot hydrophilic interfacial polymerization procedure was developed simultaneously to modify the surface property and synthesize polyamide thin film. With the procedure, a pilot scale module has a water flux of 13 LMH using a draw solution of 0.6M NaCl and a feed solution of distilled water through the design of the module configuration. © 2018 Wiley Periodicals, Inc. *J. Appl. Polym. Sci.* **2018**, *135*, 46110.

KEYWORDS: films; membranes; polyamides; separation techniques

Received 13 September 2017; accepted 25 November 2017

DOI: [10.1002/app.46110](https://doi.org/10.1002/app.46110)

INTRODUCTION

A hollow fiber (HF) membrane holds attractions with respect to structural advantages over a flat sheet membrane in packing density, spacer-free modulation, and diversity of module design.¹ Since HFs have been produced by a nonsolvent or a thermal induced phase separation, they (with pore sizes larger than several tens of nanometers) have been typically used for size sieving filtration processes (e.g., microfiltration, ultra-microfiltration, membrane bioreactor, etc.).^{2–4} Once a coating process is introduced on HFs, it can be extended to a variety of separation processes [e.g., nanofiltration, gas separation, forward osmosis (FO), or pressure-retarded osmosis].^{5–9} Among dense-coating materials based on solution-diffusion theory, polyamide (PA) has gained significant attention because its high performance has been proven by industry fields (i.e., reverse osmosis, RO) for water and wastewater treatment processes due to water crisis.^{10–13} However, there is no commercialized PA-HF module for seawater desalination because of limited operating pressures up to 70 bars. Recently, other PA-HFs for osmotic pressure-driven (OPD) process such as FO^{1,7} or pressure-retarded osmosis^{3,8} have been more intensive, because those are operated at relatively low operating pressures, and OPD/RO hybrid systems could reduce energy consumption compared to independent RO systems.^{1,2,5,8,9,14–18}

PA thin film composites (TFC) are synthesized by an interfacial polymerization (IP) method. Basically, whatever the structure or

geometry of supports are, three major steps must be performed in consecutive order: first, wetting with an amine aqueous solution; second, removing the excess amine aqueous solution; and finally, formation of an interface zone using immiscible acyl chloride solutions. The primary factors to consider for defect-free PA selective layers are the geometric position (e.g., interface zone formed above or below the top surface of a support layer) and the formation uniformity (e.g., continuous interface) of an interface zone on the porous supports.¹⁹ The interface zone for flat-sheet porous supports is relatively simply flattened by mechanical squeezing using a rubber roller or air blowing to remove excess presoaked solutions. However, since the HF has two circular structures (i.e., inside: interior cylindrical surface at lumen side, outside: exterior cylindrical surface at shell side), it is not easy to form the geometrically uniform interface zone. Of course, mechanical methods used for flat-sheet supports could be used to remove excess aqueous solutions at the outside surface of the HF if the single strand is continuously supplied. Nevertheless, there is no lab-scale report about the processing of continuous outside IP, because the tension must be constantly maintained without any broken and elongated HFs.

Typically, IP for HFs has been performed after modulation (or potting). It has advantages that this can make small-scale (i.e., less than several number of strands) HF module tests possible

Additional Supporting Information may be found in the online version of this article.

© 2018 Wiley Periodicals, Inc.

inside or outside (i.e., useful to optimize reaction conditions). However, it would be difficult to conduct the outside IP processing when the number of HF strands increases. For defect-free PA coating, all the interface zones must be independently separated. At a high packing density (i.e., HF's surface area per module volume or HF's area per module foot print), it would be difficult individually to separate all the strands in a module after wetting because of capillary contacts among the strands.¹⁶ As an alternative option, if the interface zones are formed inside, it can form solely in all the HF strands in modules regardless of packing density. Also, the inside PA-TFC-HFs could be more favorable with respect to mass transfer or energy consumption than the outside PA-TFC-HFs due to frictional and kinetic pressure losses along the HF's.^{9,18} Therefore, the inside IP would be suitable to fabricate large-scale PA-TFC-HF modules.

Veríssimo *et al.* described a practical manufacturing method for preparing an inside PA-TFC on a single strand HF.¹⁷ The procedure is as follows: (1) a wetting stage with the aqueous solution; (2) a gas purging stage to remove excess an aqueous solution; and (3) the flow of the organic solutions through the lumen side.¹⁷ Until recently, the method has been widely used in small-scale modules. However, there are several limitations in expanding to large-scale HF's. First, the aqueous solution must be uniformly soaked on/in all the HF's. When the aqueous solution is pumped into the lumen side, a pressure difference among HF's could take place because the cutting face of the HF's at the potting area is irregular and HF's are typically randomly packed.¹⁵ Since the pressure deviation results in nonuniform wettability of aqueous solutions, PA-TFC performance varies among HF's. Like the wetting stage, the pressure deviation can also occur at the gas purging stage. It is more serious because it induces the deviation of concentration as well as interface zone. To solve the irregular wetting and purging issues, Sun and Chung studied a direct soaking method.¹⁶ They prepared 50 strands of HF's without housing (i.e., a nude type module). The nude type module was directly immersed in an aqueous solution, and then a vacuum was applied to the lumen side to maintain a transmembrane pressure. Finally, the module was transferred and immersed in organic solutions. Although the method could resolve the pressure deviation during the wetting, it would be impossible for the inside interface zone due to the nude type module (i.e., vessel-less module). Therefore, this study focused on how to perform inside IP with uniform performances (i.e., valuable water flux and salt rejection) on large-scale HF modules.

In addition, for the OPD process, supports must have hydrophilic surface properties to enhance the mass transfer from low to high saline solutions.¹⁷ Polydopamine (PDA) has been recognized as an attractive surface modification material for water-based processing due to its intrinsic hydrophilicity and antifouling abilities.^{20–22} Typically, PDA is precoated on/in supports via self-oxidation before IP. However, this general method increases the unit cost of production or requires additional production facilities. Therefore, this study suggests a one-pot hydrophilic IP procedure to solve limitations of PDA coating.

Quality control of each module must be also considered. Defects in PA-HFs are detected via a gas bubbling test.²³ However, since for large-scale HF's, it would be impossible to monitor or fix one at a time, another real-time quality control must be developed. Herein, a one-pot hydrophilic IP procedure provides one solution to detect IP coating uniformity, by which one can directly observe the coating uniformity by comparison of the PDA color (dark brown) on the HF's. Using the one-pot hydrophilic IP procedure, we systematically studied various approaches to produce inside PA-TFC-HF modules.

EXPERIMENTAL

Materials

For IP monomers, *m*-phenylenediamine (MPD) and trimesoyl chloride (TMC) were purchased from Sigma-Aldrich Co. (St. Louis, MO, USA). *n*-Hexane for the organic phase and methanol for cleaning were purchased from Ducksan Chem. Co. (HPLC grade, South Korea). Dopamine (DA) as a surface modification agent and Tris buffers [tris acid (tris[hydroxymethyl]aminomethane hydrochloride) and tris base (tris[hydroxymethyl]aminomethane)] as a pH buffer were purchased from Sigma-Aldrich Co. (St. Louis, MO, USA). All the chemicals were used without any purification. Polyacrylonitrile (PAN, MWCO = 30,000 kDa, HiSep UF grade) HF was used as a main support (see in Supporting Information Table S1).

Membrane Preparation

The one-pot hydrophilic IP procedure was developed and optimized using a single PAN HF. First, a single HF was washed with distilled water three times. After draining water, HF's were immersed into the MPD aqueous solution of 2 wt %. The soaking time of MPD solutions without DA was 30 min. The pH of MPD aqueous solutions was adjusted using Tris buffers (0.05M) as described in Supporting Information (Table S2). The concentration of DA was controlled from 0 to 0.25 wt %. The soaking time of MPD/DA solutions was in the range of 30 and 120 min due to DA reaction. The excess MPD or MPD/DA solutions on the HF surface was gently removed with a sponge. The HF's were immersed into TMC solutions of 0.2 wt % with *n*-hexane. After IP reactions for 10 min, the HF was cleaned with fresh *n*-hexane several times. The PA-TFC-HFs were post-treated in a convection oven at 80 °C for 5 min. After that, the PA-TFC-HF (effective length: 20 cm) was modulated with a stainless steel pipe. After full curing (3 h), the single PA-TFC-HF module was stored in distilled water until utilization.

A 2-inch HF module was vertically installed in a home-made inside coating equipment [see Supporting Information Figure S1(a)]. The inside coating equipment consisted of a digital pressure sensor (SENSYS, Japan), a peristaltic pump (Cole-Parmer with a 77200-62 head), and an inline filter (Whatman, pore size 200 nm, PTFE). The digital sensor was installed at the module inlet of the organic solution pathway. The inline filters were mounted on the module inlets of each solution pathway. To prepare 2-inch PA-TFC-HF modules, the concentrations of MPD solutions in pH 9 and TMC solutions were 2 and 0.2 wt %, respectively. DA (0.05 wt %) was dissolved in MPD solutions before wetting or replacing into a module. For finding the suitable inside IP coating, four processes were tested (Table I).

Table I. Various Strategies for Inside IP Coating

	Procedure	Illustration of IP procedure	Issues
Method 1 (typical IP method)	(1) Circulation of MPD solutions (lumen side). (2) Removing excess MPD solutions (lumen side). (3) Circulation of <i>n</i> -hexane (lumen side). (4) Circulation of TMC solutions (lumen side)		Same issue as method 2
Method 2 (nude module coating)	(1) Circulation of MPD solutions (lumen side). (2) Removing excess MPD solutions (lumen side). (3) Circulation of <i>n</i> -hexane (lumen side). (4) Circulation of TMC solutions (lumen side)		
Method 3 (vacuum assistance method)	(1) Circulation of MPD solutions (lumen side). (2) Vacuum connected to the vessel orifice after blocking the others. (3) Circulation of <i>n</i> -hexane. (4) Circulation of TMC solutions		
Method 4 (co-flowing method)	(1) Circulation of distilled water (lumen side). (2) Circulation of <i>n</i> -hexane (lumen side). (3) Filling MPD solutions (shell side). (4) Circulation of TMC solution (lumen side)		

Briefly, method 1 was a typical IP coating with housed HF module; (1) prepared MPD/DA solutions were circulated through lumen sides under the inlet flow pressure of 100 mbar for 30 min, (2) excess MPD/DA solutions were removed using N_2 gas (100 mbar) for 5 min, (3) *n*-hexane was circulated through the lumen side for 10 min, (4) replaced TMC solutions were circulated through the lumen side for 10 min, (5) finally, methanol was fulfilled in the module before utilization. Method 2 was almost same to method 1 except for use of vessel-less modules (named nude modules). Method 3 (termed vacuum assistance) was as follows: (1) MPD/DA solutions were circulated through lumen sides under the inlet flow pressure of 700 mbar for 30 min, (2) three orifices (two lumen sides and one vessel side) was blocked, a vacuum pump was connected to the last vessel orifice, (3) *n*-hexane was circulated through the lumen side under vacuum pressure of -500 mbar until finish the IP, (4) replaced TMC solutions were circulated through the lumen side for 10 min, (5) finally, methanol was fulfilled in the module before utilization. Method 4 (named co-flowing IP) was as follows: (1) distilled water was circulated through the lumen

side under the inlet flow pressure of 700 mbar for 10 min, (2) distilled water was replaced with *n*-hexane under the inlet flow pressure of 700 mbar for 10 min, (3) MPD/DA solutions were circulated through the shell side at 20 mL/min for 30 min, (4) after that, TMC solutions were replaced with *n*-hexane under the inlet flow pressure of 700 mbar for 10 min, (5) finally, after moving all the solutions existing inside and outside HF, methanol was fulfilled in the module before utilization. The co-flowing inside IP process was directly used for preparing 4-inch PA-TFC-HF modules. The inner diameter of orifices mounted on 4-inch HF modules was 1/2 inch. The axial distances between orifices mounted on the vessel of 4-inch HF modules were 10 cm.

Characterization and Simulation

The morphologies of samples after Pt sputter coating were observed using a Hitachi SEM 4400 model (Japan). The functional bonding of reacted PA was analyzed using a JASCO 4600 (USA) FTIR spectrometer. The UV-vis absorption peaks of solutions were measured using a DR6000 HACH (USA) to indicate

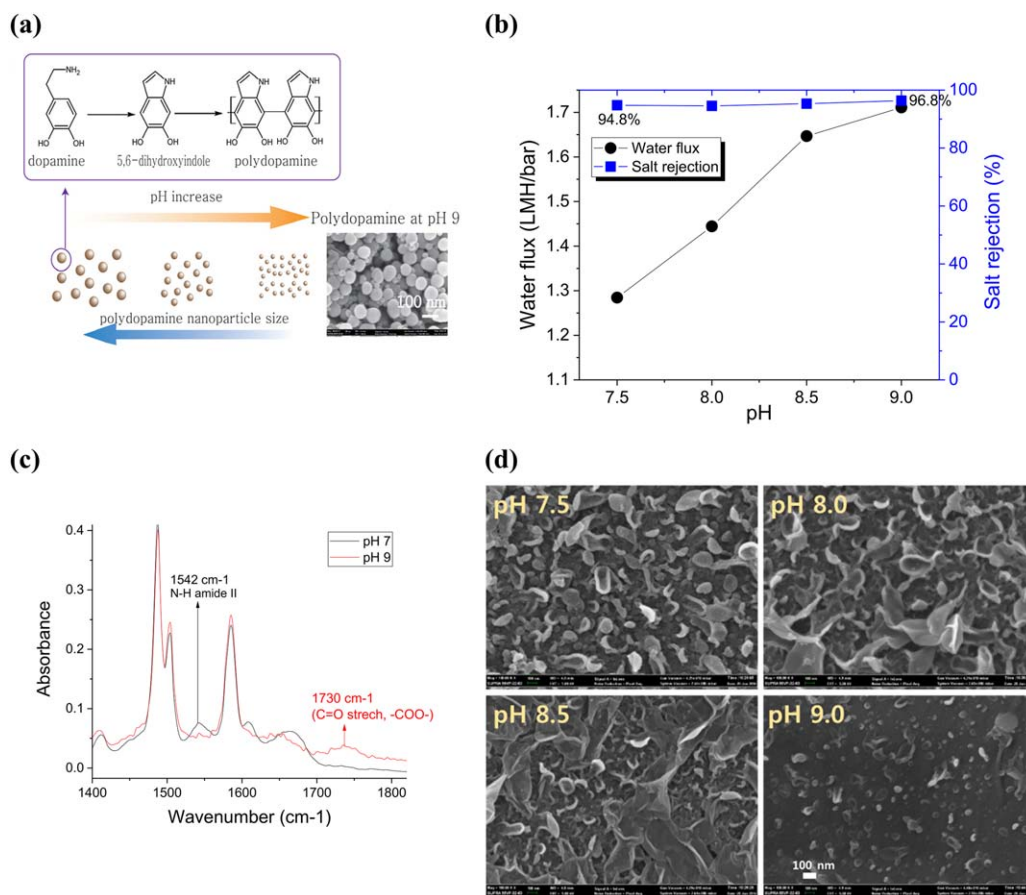


Figure 1. (a) Schematic illustration of self-oxidation polymerization dependence of dopamine on pH. (b) The water flux and salt rejection as a function of pH. (c) FTIR spectra of PAs synthesized at pH 7 and 9. (d) Surface SEM images of PA synthesized in a variety of pH. [Color figure can be viewed at wileyonlinelibrary.com]

the oxidation of DA. The computational fluid dynamic was performed using a Solidworks software (USA) with the Flow Simulation package. The module design was simplified; the number of HF was 100, the fluid material was distilled water, a temperature was 25 °C, the flow pattern was laminar flow, the outlet pressure was atomic pressure, the flow rate was 100–500 mL/min, the length of a module was 400 cm, and the diameter of a module was 6 cm. The water flux and reverse salt flux were not considered.

Membrane Performance

The intrinsic water flux (LMH/bar) was measured by weighing the permeated water with 0.2 wt % NaCl solutions at 5 bar for 30 min [$=Q/(A_m \cdot t \cdot p)$; Q is the permeated water weight, A_m is the area of membrane, p is applied pressure, and t is the time]. Salt rejection was calculated by measuring permeate (C_p)/feed (C_f) conductivities using a Mettler Toledo (USA) with an InLab 738-ISM sensor [$= (1 - C_p/C_f) \times 100\%$]. For OPD tests, a draw solution of 0.6M NaCl and a feed solution of distilled water (50 μ S/cm) were pumped into the PA-TFC-HF modules. Back pressure regulators (Parker) were installed at each pipe to make the flow pressure equal. A draw solution was pumped in the lumen side (i.e., the active layer facing the draw solution). The water flux (J_w) was calculated by weighing the permeated water [$J_w = \Delta V/(A_m \cdot t)$; ΔV is the volume change of the feed

solution over times in the duration time (t) of the tests, and A_m is the area of the membrane].

RESULTS AND DISCUSSION

One-Pot Hydrophilic IP Procedure

PDA has been widely used to modify hydrophobic substrates.^{3,20} The mechanism of surface modification is based on self-oxidation polymerization of DA with the catechol functional groups.²⁴ The self-oxidation occurs in the alkaline environment that directly influences the nanoparticle sizes of aggregated PDA, as illustrated in Figure 1(a).²⁵ To create an alkaline environment, Tris buffers in this study were used.

Before studying DA addition effects during IP, we observed the pH effect on the performance of PA-TFC-HFs. The water flux increases and the salt rejection slightly increases as the pH increases. Liu *et al.* studied the pH effects on PA-TFC performance.²⁶ They showed that the increase in the pH accelerates reactions between amine and acyl chloride by neutralizing the hydrogen chloride. The enhanced reaction increases the thickness of the PA layers so that the water flux declines. However, this study observed different results that the water flux increases with increasing in the pH, as shown in Figure 1(b). The FTIR data [Figure 1(c)] indicate that the PA-TFC has shown a C=O stretching peak at 1730 cm⁻¹ at pH 9, while it has more intense peaks of

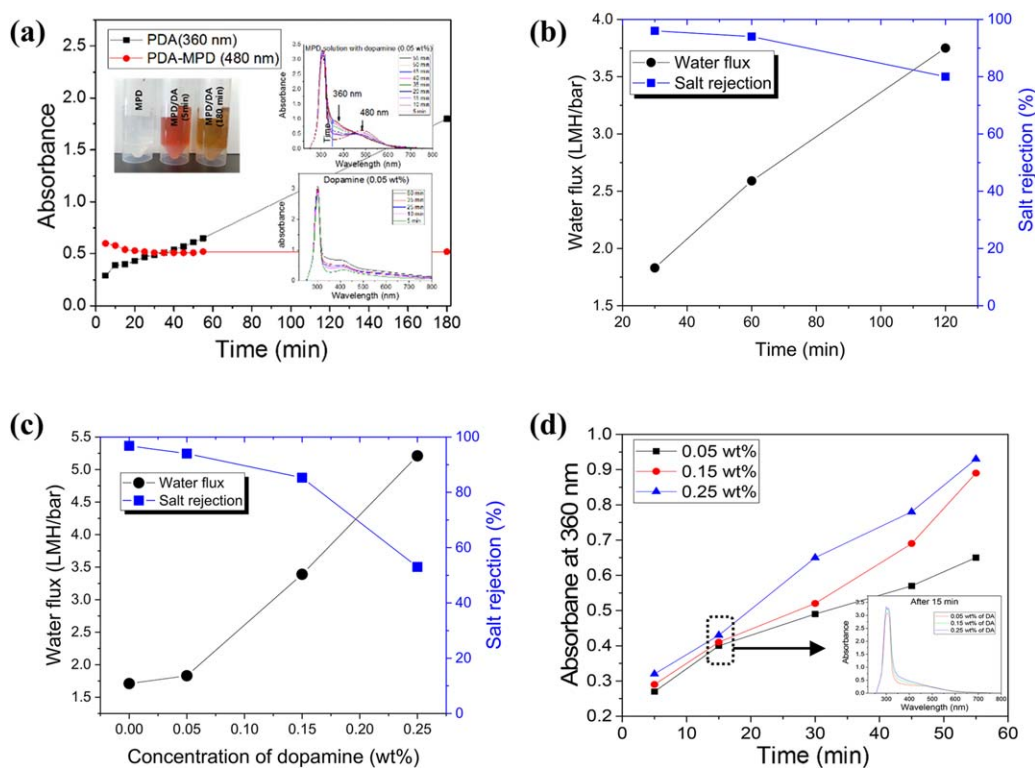


Figure 2. (a) UV-vis absorbance at 360 and 480 nm of MPD/DA solutions as a function of preparing time. The insert graphs are UV-vis spectra of MPD/DA and DA without MPD. (b) Water flux and salt rejection as a function of preparation time. (c) Water flux and salt rejection as a function of DA concentration. (d) UV-vis absorbance at 360 nm for MPD/DA solutions as a function of preparation time. The inserted image responds to UV-vis spectra when the solutions were prepared after 15 min. [Color figure can be viewed at wileyonlinelibrary.com]

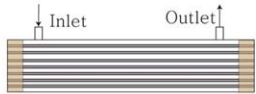
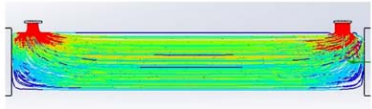

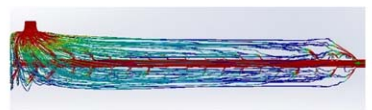

amide II at 1542 cm^{-1} at pH 7. This means that the PA-TFC at pH 9 has more carboxylic acid functionality. In Werber *et al.* reported on post-treatment effects on PA performance,²⁷ a post-treatment with ammonium hydroxide shows the improved performance. Lind *et al.* showed a similar result with NaHCO_3 as a postchemical treatment agent.²⁸ Similarly, the increase of the pH in our data might enhance residual carboxylic acid functionality. The increased carboxylic acid could influence on the morphology of PA surface as presented in Figure 1(d). The size of ridge-and-valley increases with increasing in pH, while becomes smaller at pH 9. Those morphological changes on pH might results in the enhanced water flux.

Using the Tris buffer of pH 9, the concentration of DA was optimized. Xu *et al.* recently reported a similar method.²⁹ They examined PA-TFC performance when DA was directly incorporated into MPD solutions. The chemical reaction between catechol and amine depends on the pH. At the pH below 7, since there is no chemical bonding between them, the incorporation of DA increases the water flux, while decreases salt rejection due to loose cross-linking between DA and TMC. However, at higher than pH 8.5, DA is self-oxidized into PDA. The PDA consequently interacts with amines of MPD due to Michael addition.³⁰ Interacted PDA-MPD enhances the PA-TFC performance without a color change for 180 min. However, our data present that DA was continuously self-polymerized into melanin, which indicated by the absorption spectrum at 425 nm, as shown in Figure 2(a). When DA was mixed with MPD

solutions, completely different peaks were observed. An absorption spectrum at 480 nm was observed at the initial stage, and the absorbance intensity slightly decreased up to 30 min, and then maintained for 180 min. But another spectrum at 360 nm was stronger over time. The peak comes from the compounds synthesized by Michael addition or Schiff base reaction between the quinones in PDA and the amines in MPD.²⁹ Also, the color of the solution became a darker brown, in contrast to Xu *et al.*'s observations.²⁹ This means that the self-oxidation of DA with MPD continuously occurs.³¹ Figure 2(b) shows the water flux and salt rejection as a function of preparation time for the MPD/DA solution. The longer the preparation time, the more the water flux increases (while salt rejection decreases). These results could correspond to an intensity increase in the absorption spectrum at 360 nm. That is, the concentration of free MPD might decline with increasing in the preparation time.^{3,19}

The existence of reactions between PDA/DA and MPD could be critical to the performance of PA-TFC. Figure 2(c) shows that the water flux increases with increasing in the concentration of DA. The increase of DA concentration in the MPD solutions does not change the absorption spectrum at 480 nm, while the absorption spectra intensities at 360 nm increases, as shown in Figure 2(d). As in the results for the preparation time, the increase of DA concentration promotes the reaction between quinones of PDA and amines of MPD.²⁹ Consequently, the water flux increases with increasing in the concentration of DA.

(a)

Name	Configuration of inlet/outlet orifice	CFD
Type 1	 <p>Inlet orifice : 1, outlet orifice : 1</p>	
Type 2	 <p>Inlet orifice : 80, outlet orifice: 1</p>	
Type 3	 <p>Inlet orifice : 80, outlet orifice: 12</p>	N.A.

(b)

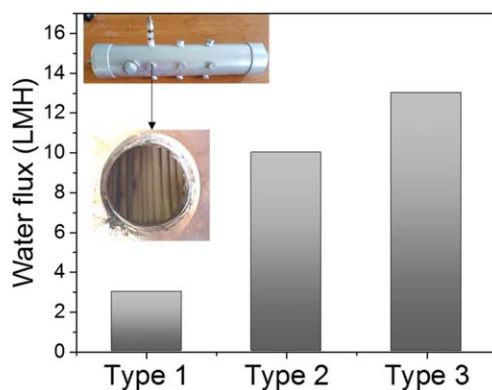


Figure 3. (a) Schematic illustration of various inlet/outlet configurations for 4-inch HF modules. (b) OPD water flux of 4-inch size HF modules. [Color figure can be viewed at wileyonlinelibrary.com]

Optimization of inside IP Coating for 2-Inch Size HF

The one-pot hydrophilic IP procedure has another advantage that it is able to directly visually observe the concentration deviation during soaking MPD/DA solutions. Many reports indicated that the concentration of MPD significantly influences the performance of active layer.^{3,19} If the deviation of MPD/DA concentrations occurs, the color among HF strands is different. As shown in Table I, when a nude HF module (method 2) was used with a typical coating method, the color among the HF was clearly different. As mentioned, when the aqueous solution was pumped into the lumen side, a pressure deviation based on fluid dynamics could take place due to a nonuniform packing distribution of the HF.¹⁵

One of the simple approaches to solve the nonuniform wetting is to increase the flow rate of the MPD solutions until it occupies the shell volume in a HF module. After draining the penetrated MPD solutions in the shell side, all the HF had the uniform brown color. The complete wetting approach would be suitable for minimizing the concentration deviation. The next

consideration is how to remove excess MPD solutions. There are two approaches; nitrogen gas purging (method 1) and a vacuum assistance (method 3). Use of nitrogen gas could similarly induce nonuniformity among HF as the deviation problems occurred during the MPD circulation.¹⁶ The lack of uniformity induces a geometry position difference in the IP zones, which more seriously affects the performance of the PA-TFC.³² Also, when the nitrogen gas purging was not sufficient, PA active layers were taken off when draw or feed solutions flow along PA coating faces. Conversely, when the purging was too strong and long, and defective PA was synthesized due to dewetting of MPD solutions on hydrophobic supports.

As another solution approach, the vacuum assistance method (method 3) was considered. After complete wetting of the MPD solutions, when a vacuum was applied in the shell side, the excess MPD was drained. The vacuum pressure is a critical factor to control a geometry position in the IP zones. When liquid filled the pores of a porous medium, it was retained by capillary

forces, depending up the interfacial tension (γ), contact angle (θ), and pore diameter (D). According to Jurin's Law, the maximum applied pressure is estimated as follows:

$$\Delta P = \frac{4\gamma \cos\theta}{D} \quad (1)$$

The pore size of the PAN used is about 3 nm.³³ On the other hand, the burst bubble pressure is around 700 mbar. Therefore, the vacuum pressure was set at -500 mbar. After that, *n*-hexane was circulated before IP to pressurize the remaining MPD solution on the surface in the lumen side as described by a Verissimo *et al.*'s method.¹⁷ The TMC solution was consequently circulated. After IP for 10 min, *n*-hexane was recirculated to remove unreacted TMC. Although the vacuum assistance IP seem to solve the inside IP coating issue, another problem exists: the MPD/DA/PDA relict around the potting faces, as shown in Table I (method 3). When MPD solutions were pumped into the lumen side, those materials were coated on all the surfaces. Since they acted as foulants, an additional cleaning processes must be integrated after IPs (i.e., increase the production cost).

To minimize the cleaning issue, we developed a co-flowing IP procedure. First, to form the interface zone in the lumen side, distilled water was circulated and filled in all the pores. Then *n*-hexane was circulated to fill the lumen side. The flow rate of *n*-hexane is critical to induce the geometrical interface zone. Therefore, the best option to find the optimized flow rate is to install a digital pressure sensor to monitor the inside pressure. The maximum pressure (or flow rate) must be lower than the value of eq. (1). At this time, the water trapped in pores might hinder the wetting of *n*-hexane. The MPD solution was filled in the shell side, and deposited for 30 min. The time was suitable for replacing pore-filled distilled water into the MPD solutions and modifying the surface property via PDA.³ Finally, *n*-hexane was replaced by TMC solutions. The co-flowing IP procedure solved the current hurdles; uniformly IP coating and washing processing minimization.

Module Performance and Vessel Design of 4-Inch PA-TFC-HFs

PA-TFC-HF modules prepared by the co-flowing IP procedure with the one-pot hydrophilic IP procedure (Supporting Information) were tested for OPD processes. The draw solution was allowed to flow through the lumen side. If there is no reverse salt flux, the external concentration is negligible. However, since there are no perfectly salt-rejecting membranes, the flow dynamic of the feed/draw solutions must be considered. As shown in Figure 3, we tested configurations and positions of inlet/outlet orifices. A type 1 HF module has each inlet and outlet in the same direction, as indicated in Figure 3(a). The water flux of the HF modules has 3 LMH as presented in Figure 3(b). A Hydration Technology Innovations (HTI's) CTA FO membrane has the water flux of 9 LMH (1M NaCl), but the TFC FO membrane has 20 LMH.³⁴ Similarly, the 8 inch spiral FO modules supplied from Toray Chemical Co. has the water flux of 17–30 LMH.³⁵ However, type 1 HF modules were lower than the commercialized type. One reason is the external concentration polarization due to a reverse salt flux from high to low

concentration. If the fresh feed water is not sufficiently supplied, the external concentration polarization critically results in the OPD performance. The increased external concentration polarization dramatically reduces the efficient osmotic pressure so that the water flux decreases. There are two approaches to solve the concentration polarization issues for large-size modules. One is the position/configuration of inlet orifices; as the inlet orifice is located at the center of HF modules, the feed water must penetrate across the HFs into the outlet orifice, as indicated in Figure 3. Also, if the number of inlet orifices is one, the effect of reducing the external concentration polarization will be insufficient. Therefore, as the number of inlet orifices increased up to 80 orifices (type 2 HF), the water flux increased about threefold over type one HFs. This result indicates that reducing the distance of the feed water pathway between inlets and outlets is important in increasing the water flux. When the number of vessel orifices increased as for type 3, the type 3 HF has about 13 LMH. Our OPD modules shows similar performance to that of Jian's modules (the number of HF strands: 300, area of membrane: 0.18 m²).³⁶

Since the water flux of the type 3 HF is still lower than that of the commercialized spiral FO modules, additional studies needs to be done to improve OPD performance. The spiral type modules have spacers to reduce external concentration polarization which induces turbulence flowing. That is, the module design based on the flow dynamic must be further studied to enhance the water flux. However, as the inserted images in Figure 3(b), the distances among HFs are not enough for feed water to flow across surfaces of the HFs due to relatively high packing density (ca. 50%). Thus, the packing density must be optimized with the processing flow rate, as Wan *et al.*'s results.²³ Another prospective study is the structure parameter of HF. HF used in this study has relatively thick wall (ca. 700 μm in thickness) compared to flat sheet membrane (thinner than 100 μm in thickness), as the thickness is directly related to the structure parameter that influences on the internal concentration polarization.³⁷ Therefore, although the current greatest hurdle in producing inside PA-HFs is solved from this study, the two issues presented in the near future must be resolved inevitably.

CONCLUSIONS

This study presents a practical method for fabricating PA-TFC-HF membranes via IP for commercial utilization in OPD processes. To reduce the production costs and improve performance for the ODP process, a one-pot hydrophilic coating procedure was developed. With this procedure, we successfully produced inside PA using the co-flowing IP method. The methods were directly applied to large size HF modules. With studying the module configuration to minimize the external concentration polarization, the performance of 4-inch PA-TFC-HF modules has 13 LMH of water flux. To improve the expected HF performance, we are still developing the configuration of modules as well as optimized HFs with the PHILOS Company (Korea) in order to release the OPD module on the global market.

ACKNOWLEDGMENTS

This work was supported by the technological development support program (B6-5516) funded by the National Research Council of Science & Technology (Korea). We thank Synopex Co. (Korea) for supplying the PAN HF modules.

REFERENCES

1. Minier-Matar, J.; Santos, A.; Hussain, A.; Janson, A.; Wang, R.; Fane, A. G.; Adham, S. *Environ. Sci. Technol.* **2016**, *50*, 6044.
2. Bonyadi, S.; Chung, T. S.; Krantz, W. B. *J. Membr. Sci.* **2007**, *299*, 200.
3. Ingole, P. G.; Kim, K. H.; Park, C. H.; Choi, W. K.; Lee, H. K. *RSC Adv.* **2014**, *4*, 51430.
4. Lidén, A.; Persson, K. M. *J. Water Supply Res. Technol. Aqua* **2016**, *65*, 43.
5. Zhou, B.-W.; Zhang, H.-Z.; Xu, Z.-L.; Tang, Y.-J. *Desalination* **2016**, *394*, 176.
6. Ingole, P. G.; Choi, W. K.; Baek, I.-H.; Lee, H. K. *RSC Adv.* **2015**, *5*, 78950.
7. Luo, L.; Wang, P.; Zhang, S.; Han, G.; Chung, T.-S. *J. Membr. Sci.* **2014**, *461*, 28.
8. Cheng, Z. L.; Li, X.; Liu, Y. D.; Chung, T.-S. *J. Membr. Sci.* **2016**, *506*, 119.
9. Han, G.; Wang, P.; Chung, T.-S. *Environ. Sci. Technol.* **2013**, *47*, 8070.
10. Choi, W.; Jeon, S.; Kwon, S. J.; Park, H.; Park, Y.-I.; Nam, S.-E.; Lee, P. S.; Lee, J. S.; Choi, J.; Hong, S.; Chan, E. P.; Lee, J.-H. *J. Membr. Sci.* **2017**, *527*, 121.
11. Fritzmann, C.; Löwenberg, J.; Wintgens, T.; Melin, T. *Desalination* **2007**, *216*, 1.
12. Gu, J.-E.; Lee, S.; Stafford, C. M.; Lee, J. S.; Choi, W.; Kim, B.-Y.; Baek, K.-Y.; Chan, E. P.; Chung, J. Y.; Bang, J.; Lee, J.-H. *Adv. Mater.* **2013**, *25*, 4778.
13. Park, S.-J.; Ahn, W.-G.; Choi, W.; Park, S.-H.; Lee, J. S.; Jung, H. W.; Lee, J.-H. *J. Mater. Chem. A* **2017**, *5*, 6648.
14. Bamaga, O. A.; Yokochi, A.; Zabara, B.; Babaqi, A. S. *Desalination* **2011**, *268*, 163.
15. Mat, N. C.; Lou, Y.; Lipscomb, G. G. *Curr. Opin. Chem. Eng.* **2014**, *4*, 18.
16. Sun, S.-P.; Chung, T.-S. *Environ. Sci. Technol.* **2013**, *47*, 13167.
17. Veríssimo, S.; Peinemann, K. V.; Bordado, J. *J. Membr. Sci.* **2005**, *264*, 48.
18. Yoon, S.-H.; Lee, S.; Yeom, I.-T. *J. Membr. Sci.* **2008**, *310*, 7.
19. Park, C. H.; Bae, H.; Kwak, S. J.; Jang, M. S.; Lee, J.-H.; Lee, J. *Macromol. Res.* **2016**, *24*, 314.
20. Lv, Y.; Yang, H.-C.; Liang, H.-Q.; Wan, L.-S.; Xu, Z.-K. *J. Membr. Sci.* **2015**, *476*, 50.
21. Vasselbehagh, M.; Karkhanechi, H.; Mulyati, S.; Takagi, R.; Matsuyama, H. *Desalination* **2014**, *332*, 126.
22. Zhang, R.; Su, Y.; Zhao, X.; Li, Y.; Zhao, J.; Jiang, Z. *J. Membr. Sci.* **2014**, *470*, 9.
23. Wan, C. F.; Li, B.; Yang, T.; Chung, T.-S. *Sep. Purif. Technol.* **2017**, *172*, 32.
24. Lee, H.; Dellatore, S. M.; Miller, W. M.; Messersmith, P. B. *Science* **2007**, *318*, 426.
25. Ho, C.-C.; Ding, S. J. *J. Mater. Sci.: Mater. Med.* **2013**, *24*, 2381.
26. Liu, M.; Yu, S.; Tao, J.; Gao, C. *J. Membr. Sci.* **2008**, *325*, 947.
27. Werber, J. R.; Bull, S. K.; Elimelech, M. *J. Membr. Sci.* **2017**, *535*, 357.
28. Lind, M. L.; Eumine Suk, D.; Nguyen, T.-V.; Hoek, E. M. V. *Environ. Sci. Technol.* **2010**, *44*, 8230.
29. Xu, L.; Xu, J.; Shan, B.; Wang, X.; Gao, C. *J. Mater. Chem. A* **2017**, *5*, 7920.
30. Zhao, J.; Fang, C.; Zhu, Y.; He, G.; Pan, F.; Jiang, Z.; Zhang, P.; Cao, X.; Wang, B. *J. Mater. Chem. A* **2015**, *3*, 19980.
31. Lv, Y.; Du, Y.; Qiu, W.-Z.; Xu, Z.-K. *ACS Appl. Mater. Interfaces* **2017**, *9*, 2966.
32. Park, S.-J.; Choi, W.; Nam, S.-E.; Hong, S.; Lee, J. S.; Lee, J.-H. *J. Membr. Sci.* **2017**, *526*, 52.
33. Giglia, S.; Bohonak, D.; Greenhalgh, P.; Leahy, A. *J. Membr. Sci.* **2015**, *476*, 399.
34. Alsvik, I. L.; Hägg, M. B. *Polymers* **2013**, *5*, 303.
35. Blandin, G.; Verliefde, A.; Comas, J.; Rodriguez-Roda, I.; Le-Clech, P. *Membranes* **2016**, *6*, 37.
36. Ren, J.; McCutcheon, J. R. *Ind. Eng. Chem. Res.* **2017**, *56*, 4074.
37. McGovern, R. K.; Mizerak, J. P.; Zubair, S. M.; Lienhard V, J. H. *J. Membr. Sci.* **2014**, *458*, 104.